

RESEARCH ARTICLE

Marginal effects of public health measures and COVID-19 disease burden in China: A large-scale modelling study

Zengmiao Wang¹ ^{*}, Peiyi Wu¹ ^{*}, Lin Wang², Bingying Li¹, Yonghong Liu³, Yuxi Ge¹, Ruixue Wang¹, Ligui Wang⁴, Hua Tan⁵ ⁵, Chieh-Hsi Wu⁶, Marko Laine⁷ ⁷, Henrik Salje², Hongbin Song⁴ ^{*}

1 State Key Laboratory of Remote Sensing Science, Center for Global Change and Public Health, Faculty of Geographical Science, Beijing Normal University, Beijing, China, **2** Department of Genetics, University of Cambridge, Cambridge, United Kingdom, **3** Beijing Center for Disease Prevention and Control, Beijing, China, **4** Center of Disease Control and Prevention, PLA, Beijing, China, **5** Translational and Functional Genomics Branch, National Human Genome Research Institute, National Institutes of Health, Bethesda, Maryland, United States of America, **6** Mathematical Sciences, University of Southampton, Southampton, United Kingdom, **7** Finnish Meteorological Institute, Meteorological Research Unit, Helsinki, Finland

 These authors contributed equally to this work.

* wangzengmiao@gmail.com (ZW); hongbinsong@263.net (HS)



OPEN ACCESS

Citation: Wang Z, Wu P, Wang L, Li B, Liu Y, Ge Y, et al. (2023) Marginal effects of public health measures and COVID-19 disease burden in China: A large-scale modelling study. *PLoS Comput Biol* 19(9): e1011492. <https://doi.org/10.1371/journal.pcbi.1011492>

Editor: David S. Khoury, Kirby institute, University of New South Wales, AUSTRALIA

Received: May 23, 2023

Accepted: September 5, 2023

Published: September 18, 2023

Copyright: © 2023 Wang et al. This is an open access article distributed under the terms of the [Creative Commons Attribution License](https://creativecommons.org/licenses/by/4.0/), which permits unrestricted use, distribution, and reproduction in any medium, provided the original author and source are credited.

Data Availability Statement: The human mobility data that support the findings of this study are available from the Baidu location-based services (<http://qianxi.baidu.com/>). Epidemiological data and code are available on the following repository: <https://github.com/peiyiw/Zero-Covid.git>.

Funding: This research was supported by a grant from the Scientific and Technological Innovation 2030 - Major Project of New Generation Artificial Intelligence (2021ZD0111201), which supported ZW; a grant from the National Natural Science

Abstract

China had conducted some of the most stringent public health measures to control the spread of successive SARS-CoV-2 variants. However, the effectiveness of these measures and their impacts on the associated disease burden have rarely been quantitatively assessed at the national level. To address this gap, we developed a stochastic age-stratified metapopulation model that incorporates testing, contact tracing and isolation, based on 419 million travel movements among 366 Chinese cities. The study period for this model began from September 2022. The COVID-19 disease burden was evaluated, considering 8 types of underlying health conditions in the Chinese population. We identified the marginal effects between the testing speed and reduction in the epidemic duration. The findings suggest that assuming a vaccine coverage of 89%, the Omicron-like wave could be suppressed by 3-day interval population-level testing (PLT), while it would become endemic with 4-day interval PLT, and without testing, it would result in an epidemic. PLT conducted every 3 days would not only eliminate infections but also keep hospital bed occupancy at less than 29.46% (95% CI, 22.73–38.68%) of capacity for respiratory illness and ICU bed occupancy at less than 58.94% (95% CI, 45.70–76.90%) during an outbreak. Furthermore, the underlying health conditions would lead to an extra 2.35 (95% CI, 1.89–2.92) million hospital admissions and 0.16 (95% CI, 0.13–0.2) million ICU admissions. Our study provides insights into health preparedness to balance the disease burden and sustainability for a country with a population of billions.

Foundation of China (82204160) that supported ZW; a grant from the National Natural Science Foundation of China (82073616) that partially supported ZW; a grant from the National Key Research and Development Program of China (2022YFC2303803, 2021YFC0863400) that partially supported ZW; a grant from the Beijing Science and Technology Planning Project (Z201100005420010) that partially supported ZW; a grant from the Beijing Natural Science Foundation (JQ18025) that partially supported ZW; a grant from the Beijing Advanced Innovation Program for Land Surface Science (110631111) that partially supported ZW; a grant from the Fundamental Research Funds for the Central Universities (2021NTST17) that supported ZW; a grant from the Research on Key Technologies of Plague Prevention and Control in Inner Mongolia Autonomous Region (2021ZD0006) that partially supported ZW; a grant from Research Council of Finland (321890) that supported ML. The funders had no role in the study design, data collection and analysis, decision to publish, or preparation of the manuscript.

Competing interests: The authors have declared that no competing interests exist.

Author summary

As China continues to be challenged by successive SARS-CoV-2 variants, rethinking population health, broader than health-care system alone, is a prerequisite for health preparedness. China has introduced several changes to its public health measures in response to evolving pandemic risk, however, the effectiveness of public health measures in controlling COVID-19 outbreaks in China and their impacts on the associated disease burden have not been quantitatively assessed at the national level. Here, we developed a stochastic age-stratified metapopulation model based on high resolution human mobility data to address these questions. Our results suggest that there's marginal effect between the testing speed and reduction in the epidemic duration. Rapid implementation of population-level testing and a short response lag would be critical if aiming at suppression of potential future SARS-CoV-2 waves in China. Furthermore, the underlying health conditions would lead to extra hospital admissions and ICU admissions, where obesity is expected to contribute to most extra hospital admissions, while hypertension could contribute to most extra ICU admissions.

Introduction

Since the first COVID-19 wave in Wuhan in 2020, China implemented the strict control strategy to combat SARS-CoV-2. This strategy successfully contained hundreds of SARS-CoV-2 outbreaks across the country and was estimated to have averted more than one million deaths in China [1,2]. However, the effectiveness of the strategy appears to have been substantially challenged by the Omicron and other highly transmissible variants. Major Omicron outbreaks occurred in Shanghai, Jilin, and Hong Kong in the spring of 2022 [3–5], and there was a rapid surge of infections across China in December 2022 after the relaxation of the strategy [6–10]. Although WHO declared end to COVID-19's emergency phase [11], the effectiveness of public health measures against Omicron-like variant is still being debated, especially with regard to the COVID-19 disease burden considering underlying health conditions in the future wave.

China's public health measures mainly includes travel restrictions between cities and testing (with contact tracing and isolation) for almost three years. These measures have been adjusted in response to the changing pandemic risk (Fig 1A). During the first wave in 2020, China banned travel to and from Wuhan and implemented strict social distancing (Fig 1A). In January 2021, China began to adopt multiple rounds of population-level testing (or screening based on the definition of European Centre for Disease Prevention and Control [12]) combined with contact tracing for rapid case identification in response to the increasing risk of imported cases caused by multiple variants of SARS-CoV-2 (Fig 1A). This change represents the key transition from passive surveillance to active surveillance in China. Over the past three years, China has developed a robust PCR testing capacity, with a daily capacity of over 100 million single tube tests, and a potential testing capacity of over one billion people per day if a 1:10 pooled testing strategy is employed [13].

The critical role of testing specific populations in pandemic control, e.g., health workers [14], quarantined individuals [15,16], and international travelers [17], has been demonstrated. Mass testing was also implemented in some countries considering the existence of presymptomatic or asymptomatic transmission [18,19], with diverse purposes (e.g., reducing the SARS-CoV-2 prevalence in Slovakia [20–22], investigating the symptoms of COVID-19 and monitoring SARS-CoV-2 prevalence in England [23,24]). Rapid and/or frequent testing (two or three times per week) has been used to mitigate the transmission of SARS-CoV-2 at large

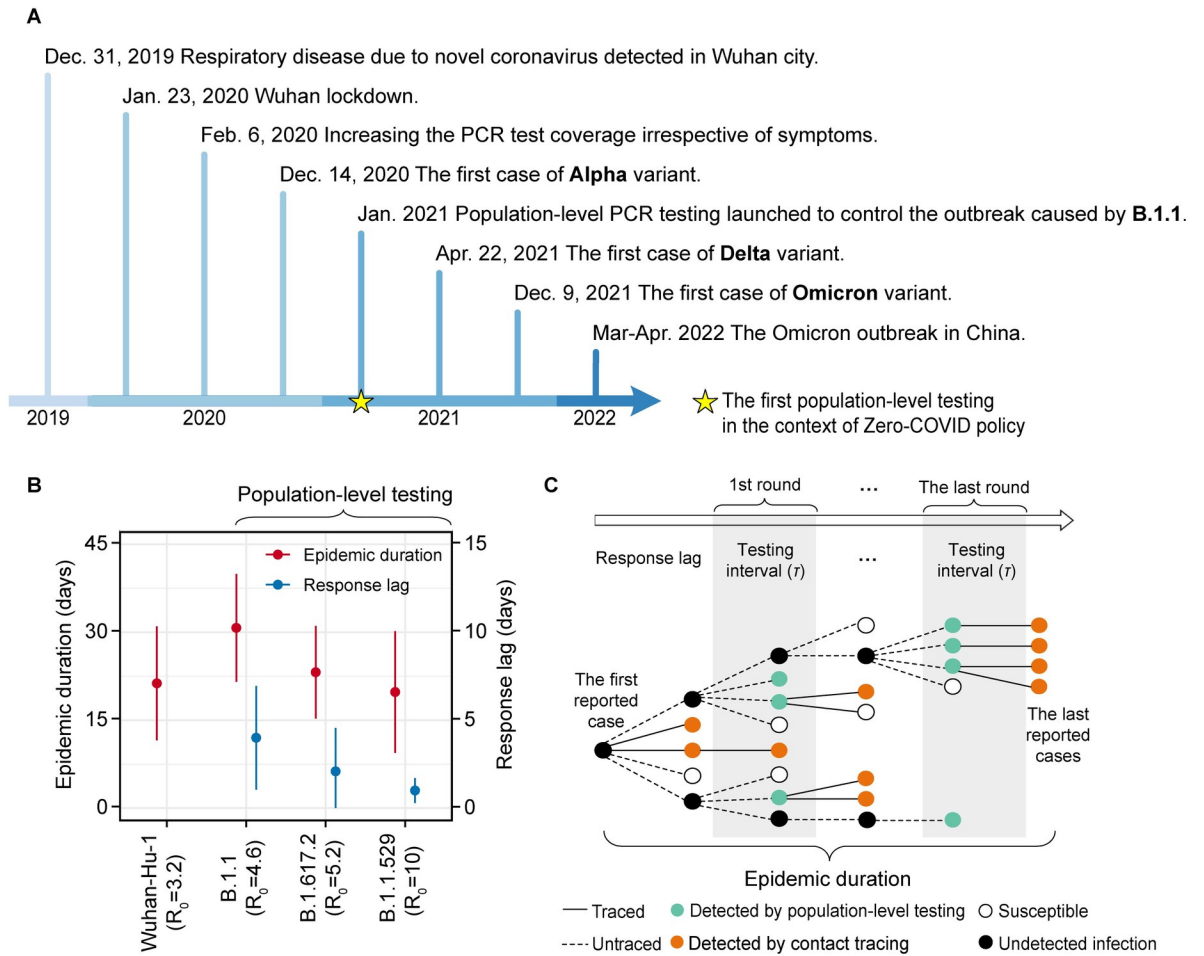


Fig 1. Evolution of the public health measures in China and successfully controlled COVID-19 outbreaks. (A) Key changes in the control strategy in China. Initial population-level testing is highlighted with a yellow star, and the first imported case of each variant of concern is in bold. (B) Successfully controlled COVID-19 outbreaks, stratified according to the SARS-CoV-2 variant causing each outbreak. From the first outbreak of B.1.1 in January 2021, multiple rounds of population-level testing were introduced. Red error bars correspond to measures of epidemic duration (i.e., time interval from the first to the last reported case in each outbreak). Blue error bars correspond to the response lag (i.e., time interval from the first reported case to the start of population-level testing at city level in each outbreak). The basic reproduction number (R_0) for Wuhan-Hu-1, B.1.1, B.1.617.2 (Delta), and B.1.1.529 (Omicron) was set to be 3.2, 4.6, 5.2 and 10, respectively, according to previous studies [31,79–81]. (C) Illustration of population-level testing and contact tracing employed in China. The testing interval is the time to finishing one round of population-level testing.

<https://doi.org/10.1371/journal.pcbi.1011492.g001>

public universities in the United States [25] and in schools and daycare facilities in Germany [26,27]. However, requirements for population-level testing have not yet been well explored in the setting of Omicron-like variant across 366 Chinese cities with human mobility [28].

Meanwhile, the travel restrictions has been extensively evaluated at different scales, from within-country [29–31] to within-continent [32] and globally [33,34]. Although the travel restrictions slowed the epidemic, they failed to stop the spread of the virus nationwide and globally [31,33,35,36]. Additionally, the potential negative effects have caused great concern [37–41], such as the association between lockdown duration and mental health [42,43]. Although the public health measures in China were relaxed to balance the advantages and disadvantages [6–8] when facing Omicron and its subvariants [44–47], few comprehensive quantitative assessments have been conducted to assess the effectiveness of control measures against Omicron variants

and the corresponding COVID-19 disease burden, especially considering the underlying health conditions and high resolution human mobility in 366 cities of China [28,48–50].

In this study, we developed a stochastic age-stratified metapopulation model to evaluate COVID-19 disease burden and public health measures for a single wave in China. We explored the feasibility of combating Omicron-like waves without implementing travel restrictions between cities. The disease burden was also assessed by considering 8 types of the underlying health conditions among the population of China. A massive nationwide mobile phone dataset covering 419 million travel movements among 366 Chinese cities before and during the pandemic was incorporated into the model. Our detailed analysis may provide insights for future pandemic preparedness based on self-monitoring and underlying health conditions in China.

Results

Population-level testing is critical if aiming at suppressing Omicron, even without travel restrictions between cities

China successfully controlled dozens of sporadic outbreaks caused by different SARS-CoV-2 variants or lineages, including B.1.1 (4 outbreaks), Delta (11 outbreaks) and Omicron (3 outbreaks), with the duration of each outbreak limited to less than a month and the maximum size of each outbreak limited to 2,500 confirmed cases (Fig 1B and S1 Table). Owing to the emergence of highly contagious Omicron variants, China substantially increased the intensity of population-level testing at city level, as measured by the shorter response lag (i.e., time interval from the first reported case to the start of population-level testing at city level in each outbreak) and testing interval (i.e., the time to finishing one round of population-level testing), compared with that for B.1.1 (Wilcoxon test statistic = 2.5, $P = 0.04$). The duration of each outbreak, as measured by the time interval from the first reported case to the last reported case, was also significantly reduced (Wilcoxon test statistics = 3, $P = 0.06$) (Fig 1B and 1C, S1 Table).

To assess the effectiveness of population-level testing at city level in controlling a highly transmissible variant like Omicron BA.1, we first developed a metapopulation model that incorporates the initial public health measures, including travel restrictions between cities and social distancing (a set of measures aiming to reduce the transmission rate, e.g., wearing masks) but without population-level testing, contact tracing and isolation. Our results reveal the difficulty in controlling a variant with similar transmissibility as Omicron using the control measures previously employed to contain the Wuhan-Hu-1 outbreak, if aiming at suppressing Omicron-like wave (S1–S7 Figs, S2 Table).

We then extended the previously developed testing–contact tracing–isolation model [51] into a stochastic age-stratified metapopulation model but without travel restrictions between cities, to assess the controllability of the Omicron-like variant in China. The study period for this model began from September 2022. The sensitivity of PCR tests when administered at different time after infection was also modelled (Section S1.3 of Supplementary Materials). Our results indicate that population-level testing with an interval of ≤ 3 days would be necessary to achieve suppression in an Omicron-like variant wave. Increasing the response lag and testing interval of population-level testing significantly extends the epidemic duration and increases the rounds of testing, resulting in more infections and a higher number of tests (Fig 2A, S8 and S9 Figs; $P < 0.001$ from the t -test in S3 and S4 Tables). The strategy with a 3-day testing interval and a response lag of 3 weeks would be least stringent among all possible combinations of control measures aiming at suppressing SARS-CoV-2 infections. Any less-stringent strategy would lead to a failure of suppression for Omicron-like wave [for example, the response lag of 4 weeks or 4-day testing interval could result in whole population isolated in many cities (S5 Table) or longer epidemic duration (S10 Fig)].

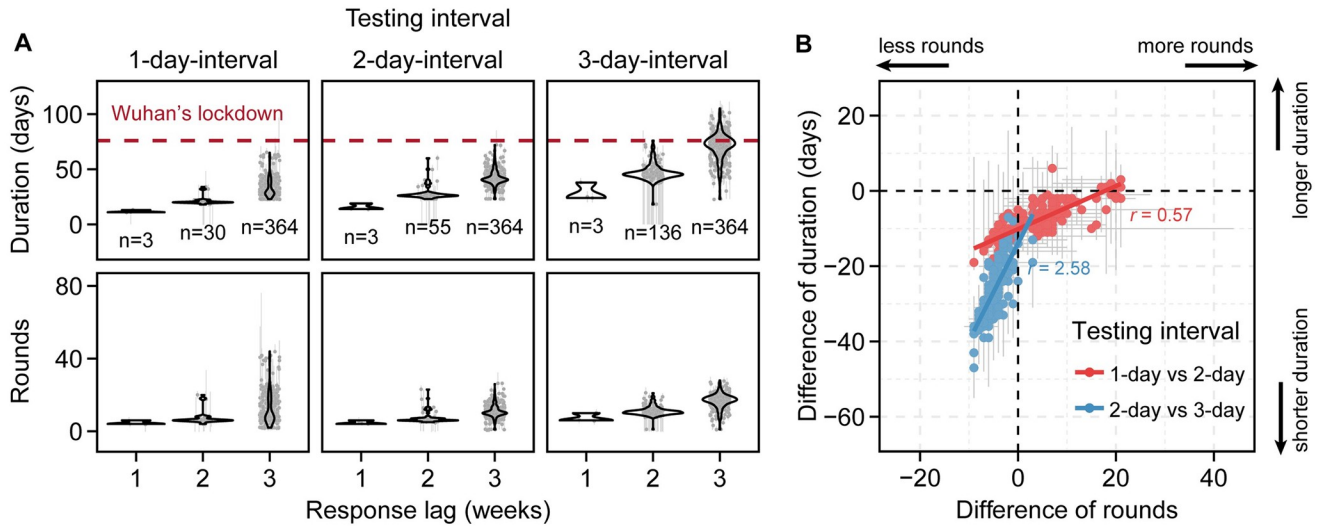


Fig 2. All possible control strategies aiming at suppressing SARS-CoV-2 infections in China during Omicron-like variant wave ($R_0 = 10$). (A) Predicted epidemic duration and rounds of testing across 366 cities in China under different testing intervals and response lags. The dashed red line shows the duration of Wuhan’s lockdown in 2020 (i.e., 76 days) as reference. The number of cities with local outbreaks is labelled below the violin plot. The grey dot represents the median and the grey error bar represents the 95% CI based on the 100 simulation. (B) Comparison of epidemic duration and rounds of testing between two successive testing intervals when the response lag was 3 weeks. A negative value corresponds to benefits yielded for duration or rounds by accelerating testing (shortened testing interval), and a positive value corresponds to potential loss for duration or rounds by accelerating testing. The slope for red dots is significantly smaller than that for blue dots ($P < 0.001$). A dot represents a city. The red and blue dots represent median and grey error bar represents the 95% CI based on the 100 simulation. The reduction of social distancing on the transmission rate was set to 18% by considering the effect of only mask wearing against SARS-CoV-2 infection [82]. The vaccine coverage for all age groups was set to 89% (consistent with 86% vaccine coverage in the ≥ 60 age group by August of 2022 in China) and the effectiveness of China’s inactivated vaccines (BBIBP-CorV and CoronaVac) against infection was set to 40% for Omicron [76,77]. The full list of epidemiological parameters is given in S6 and S7 Tables. The response lag is the time interval from the first reported case to the start of population-level testing at city level in each outbreak. The testing interval is the time to finishing one round of population-level testing.

<https://doi.org/10.1371/journal.pcbi.1011492.g002>

We observed a large number of rounds of testing for some cities with a response lag of 3 weeks and a 1-day testing interval (Fig 2A). Although suppression can be achieved in these cities for a short duration, new rounds of population-level testing may be triggered due to the importation of new COVID-19 cases from other cities. By comparison, the effect on rounds of population-level testing together with travel restrictions between cities was also evaluated; no waves were triggered by imported COVID-19 cases (S11 Fig). Sensitivity analysis showed that a SARS-CoV-2 variant with lower basic reproduction number could reduce the demand for testing, but may need fast response if testing interval is 4 days (S12 Fig). We also performed sensitivity analysis by shortening the infectious period (S13 Fig). The outbreak would be harder to control in terms of the number of cities with outbreak and the epidemic duration. Considering the emergence variants with breakthrough (e.g., BQ.1.1 and XBB), we performed sensitivity analysis to assess the feasibility of population-level testing aiming to suppress Omicron-like waves by varying the vaccine effectiveness against infection. The results showed that 3-day testing interval with the response lag of 1 week could control the outbreak even with the vaccine effectiveness against infection of 0 (an extreme situation).

Marginal effects between decreasing testing interval and reduction in epidemic duration

We observed marginal effects between the testing interval and reduction in the epidemic duration given a response lag of 3 weeks (Fig 2B). Decreasing the testing interval from 3 days to 2

days can largely reduce the rounds of population-level testing and epidemic duration (Fig 2B). However, reducing the testing interval from 2 days to 1 day only gives marginal gain, i.e., the reduction in epidemic duration decreased with a one-round increase in testing (smaller slope for 1-day vs. 2-day testing interval observed with $P < 0.001$ from the t -test, compared with that for a 2-day vs. 3-day testing interval). A similar pattern exists under different response lags (S14 Fig). To examine whether the marginal effects between the testing interval and reduction in epidemic duration is caused by the movements of COVID-19 cases among cities, we performed a similar analysis with travel restrictions between cities. The results indicated that the marginal effects persisted (S15 Fig).

Impact of the public health measures on SARS-CoV-2 Omicron burden in China

According to the above simulations, we assessed the daily hospital beds required and the daily ICU beds required during a highly contagious SARS-CoV-2 variant (like Omicron) outbreak, accounting for hospitalization and ICU admission rates for symptomatic Omicron infection in vaccinated and unvaccinated individuals (S8 Table). The control strategy was set with a 3-day testing interval and response lag of 3 weeks, which is the least stringent strategy among all possible strategies aiming at suppressing SARS-CoV-2 infections based on the simulations. Under this scenario, the average number of SARS-CoV-2 infections per 100 individuals across the cities in China would be 1.34 (95% CI, 1.19–1.50), 1.83 (95% CI, 1.63–2.03), 1.23 (95% CI, 1.10–1.36), and 0.46 (95% CI, 0.41–0.51) for the 0–19, 20–39, 40–59 and ≥ 60 age groups, respectively (S16A Fig), with 34.71 (95% CI, 24.76–48.79) million infections in total.

Considering that hospitalization and ICU admission for COVID-19 cases are highly dependent on the underlying health conditions and age, we collected the age-adjusted risk ratios of the hospitalization and ICU admission for 8 types of underlying conditions, hypertension, diabetes mellitus, chronic kidney disease, obesity, chronic obstructive pulmonary disease, asthma, chronic liver disease and cancer, and their corresponding age-specific or region-specific prevalence in the Chinese population. The highest age-adjusted odds ratio was observed in obesity for hospitalization and chronic obstructive pulmonary disease for ICU admission, while hypertension showed the highest prevalence in China (Table 1). Based on these data, the age- and region-specific prevalence and the risk ratios of the underlying health conditions were incorporated to evaluate the COVID-19 burden (Table 1 and S8 Table, see the Methods for

Table 1. Age-adjusted odds ratios (OR) for hospitalization and ICU admission of infected individuals with underlying health conditions and the prevalence of underlying health conditions in the Chinese population.

Underlying health conditions	OR for hospitalization	OR for ICU admission	Overall prevalence in China
Hypertension	2.01 [83]	2.95 [84]	0.28 ^c [85]
Diabetes mellitus	2.27 [86]	3.07 [84]	0.12 ^c [87]
Chronic kidney disease	3.4 [86]	5.32 [84]	0.11 ^a [88]
Obesity	5.82* [86]	1.43 [89]	0.05 ^c [90,91]
Chronic obstructive pulmonary disease	1.07 [92]	6.66 [84]	0.03 ^b [93]
Asthma	3.83 [86]	2.63 [86]	0.01 ^c [94–96]
Chronic liver disease	2.77 [86]	1.1 [86]	0.007 ^c [97,98]
Cancer	2.88 [86]	0.91 [86]	0.002 ^b [99]

*: hospitalizations for class III obesity

The prevalence data is an average across different groups, either age-specific^a, region-specific^b or both^c.

Note: Because of the low prevalence of underlying health conditions, risk ratio was approximated by age-adjusted OR in disease burden calculation.

<https://doi.org/10.1371/journal.pcbi.1011492.t001>

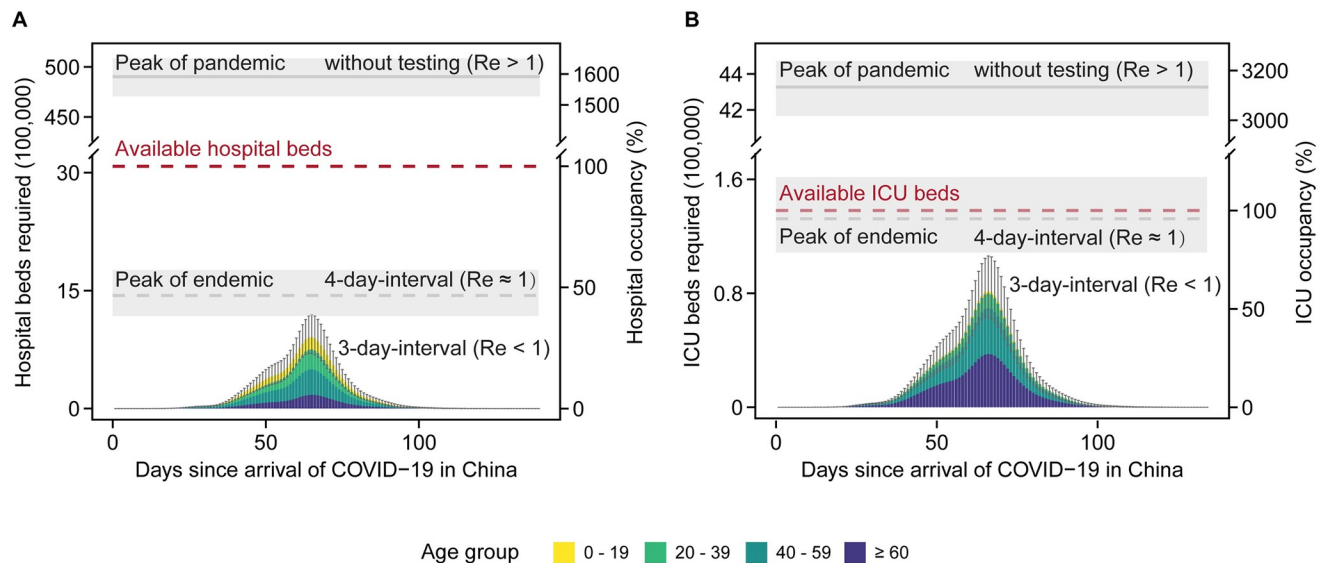


Fig 3. COVID-19 burden for the Omicron-like variant ($R_0 = 10$) under the control strategy in China. (A) Daily required hospital beds for different age groups. (B) Daily required ICU beds for different age groups. The control strategy was employed with a testing interval of 3 days and a response lag of 3 weeks (the effective reproduction number $R_e < 1$), which is the least stringent strategy aiming at suppressing SARS-CoV-2, as shown in Fig 2A. A strategy with a testing interval of 4 days and a response lag of 3 weeks would lead to the endemic of COVID-19 as shown in the grey dashed line with $R_e \approx 1$. The red dashed line represents the total available hospital beds or ICU beds in China. The grey solid line represents the peak number of required hospital beds or ICU beds during the pandemic without testing ($R_e > 1$). The bar represents the median, and the grey error bar represents the 95% CI for 100 simulations. The vaccine coverage for all age groups was set to be 89%, consistent with 86% vaccine coverage in the ≥ 60 age group by August of 2022 in China. The response lag is the time interval from the first reported case to the start of population-level testing at city level in each outbreak. The testing interval is the time to finishing one round of population-level testing.

<https://doi.org/10.1371/journal.pcbi.1011492.g003>

more details). During the outbreak projected under this scenario, both the daily required hospital beds and ICU beds for respiratory illness would be under the capacity of the health care system for respiratory illness (3.1 million hospital beds and 138,100 ICU beds in total [50,52,53]), with the highest occupancy of 29.46% (95% CI, 22.73–38.68%) and 58.94% (95% CI, 45.70–76.90%) for hospitalization and ICU beds, respectively (Fig 3). However, without testing, the peak number of daily required hospital beds would be 15.92 (95% CI, 15.28 to 16.51) times the hospital bed capacity in China (Fig 3). Even worse, the peak number of daily required ICU beds would be 31.33 (95% CI, 30.17 to 32.38) times the maximum capacity. We also evaluated the COVID-19 burden under 4-day testing interval. The endemic of COVID-19 could be reached. The required number of hospital beds would still be under capacity, but the ICU capacity may be slightly overwhelmed (Fig 3A and S17 Fig). The results still hold when taking the uncertainty in vaccine effectiveness against hospitalization and ICU admission (S18 and S19 Figs). We also performed the similar analysis based on Hong Kong-specific and Shanghai-specific age-dependent hospitalization and ICU admission rates. The COVID-19 burden would be under the capacity for 4-day testing interval (S20 and S21 Figs), demonstrating the variations in hospitalization and ICU admission rates in China.

In terms of the peak of isolated population during the outbreak, the cities with smaller population sizes and less movement, may suffer a higher proportion of isolated people than the cities with higher populations under the control strategy with a 3-day testing interval and response lag of 3 weeks (S16B Fig). The "isolated" individuals include the individuals exposed to the SARS-CoV-2 and the infected individuals. We recognize that our study did not distinguish between isolation and quarantine, as we concentrated on the percentage of individuals

who were temporarily restricted in their movements. Contact tracing in the cities with small population sizes would be another type of "lockdown", but only a few cities would experience this. The short response lag can substantially reduce the isolated population (S22 Fig), indicating the importance of fast response in cities with small populations.

The contributions of underlying health conditions

Projected by the age-stratified metapopulation model under the least stringent control strategy, 1.33 (95% CI, 1.07–1.65) million hospital admissions and 0.10 (95% CI, 0.08–0.12) million ICU admissions in total were estimated without considering the underlying health conditions (S23 Fig). After calibration for the underlying conditions (Table 1 and S8 Table, see the Supplementary Materials for more details), an extra 2.35 (95% CI, 1.89–2.92) million hospital admissions and 0.16 (95% CI, 0.13–0.2) million ICU admissions were estimated under the least stringent control strategy, corresponding to a 1.77-fold (95% CI, 1.15–2.72) and 1.67-fold (95% CI, 1.08–2.57) of that under the scenario without underlying conditions, respectively. The 40–60 age group would account for 39.96% of extra hospital admissions and the ≥ 60 age group would account for 50.30% of extra ICU admissions (Fig 4). Among the underlying health conditions, obesity could contribute to most extra hospital admissions (Fig 4A), while hypertension is expected to contribute to most extra ICU admissions (Fig 4B). Interestingly, for the 0–19 age group, obesity would account for the most extra hospital admissions among all underlying health conditions.

Discussion

China was one of the first countries to adopt the strict control strategy to control SARS-CoV-2 outbreaks in 2020. Recent adjustment of COVID-19 responses (i.e., "20 measures" and "10 new

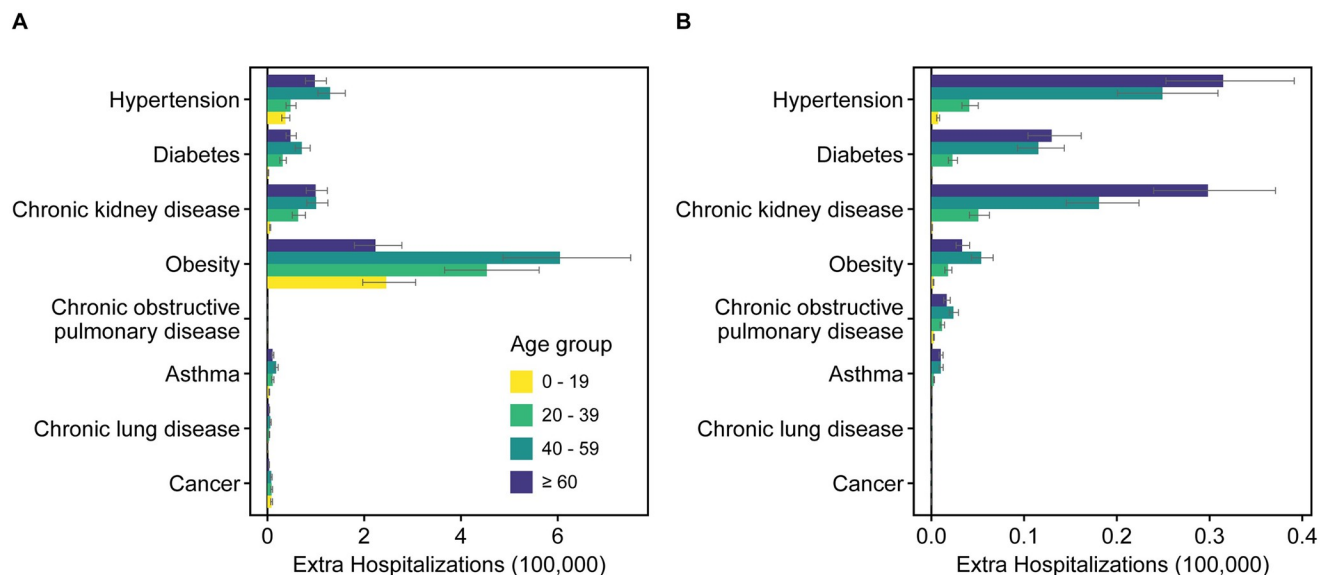


Fig 4. The COVID-19 burden contributed by the underlying health conditions under the control strategy for Omicron-like variant ($R_0 = 10$) in China. (A) The extra number of hospitalizations due to the underlying health conditions for different age groups. (B) The extra number of ICU admissions due to underlying health conditions for different age groups. The bar denotes median, and the grey error bar represents the 95% CI for 100 simulations. The extra number of hospitalizations/ICU admissions is the difference between the hospitalizations/ICU admissions considering the underlying health conditions and the hospitalizations/ICU admissions without considering the underlying health conditions. The control strategy was employed with 3 days of testing interval and 3 weeks of response lag (i.e., the least stringent control strategy). The response lag is the time interval from the first reported case to the start of population-level testing at city level in each outbreak. The testing interval is the time to finishing one round of population-level testing.

<https://doi.org/10.1371/journal.pcbi.1011492.g004>

measures") indicated the end of this strategy [6,7]. However, comprehensive quantitative assessments of the public health measures and the corresponding COVID-19 disease burden in 366 Chinese cities is still lacking. We developed a stochastic age-stratified metapopulation model to address these questions. The modelling framework allows us to assess specific implementation strategies in terms of epidemic duration, rounds of population-level testing, and public health burdens of COVID-19 considering the underlying health conditions and the high-resolution human mobility in 366 cities of China.

Our results indicate that the rapid implementation of population-level testing with 3-day testing interval and a response lag ≤ 3 weeks would be critical if aiming at suppression of potential future SARS-CoV-2 waves in China. Increasing the testing interval to 4 days would lead to endemic of COVID-19 and result in slightly overwhelming the ICU capacity. Compared with previous studies [28,48–50], the outcomes in our study is more actionable. The reported serial interval for Omicron is between 2 and 4 days [54–56]. The sensitivity analysis by lowering basic reproduction number and shortening the infectious period indicated that the serial interval/generation time, the basic reproduction number and the response lag would have impact on the testing interval required for controlling outbreaks, but the generation time/serial interval should contribute most. Considering the fast evolution of SARS-CoV-2 and the importance of the generation time/serial interval [57], these key epidemiological parameters should be monitored continually [58], by contact tracing [59,60] or sequencing data [61].

Given the negative effects of lockdown on lifestyle and mental health [38,39], population-level testing has been proposed as a critical component of the public health measures in China, with relatively minor disruption to daily life. Testing capacity may be an issue for low- to middle-income regions. Rapid antigen testing may be an alternative solution [62], with high frequency and short turnaround time to compensate for the lower sensitivity compared with PCR tests [63–65]. A previous study showed that home antigen test sensitivity was 64% compared with same-day RT-PCR [66]. If 3-day interval is applied to PCR test, 2-day interval [$1/(3 \times 0.64) = 0.52$, that is about 2-day interval] would have to be used for rapid antigen test. Optimal pooled testing strategies can also be used in regions with limited resources [67,68]. Additionally, various rapid methods of screening and diagnosis of SARS-CoV-2 have recently been developed, for example, the Lolli-method (effective high-throughput RT-qPCR [26]), ADESSO (Accurate Detection of Evolving SARS-CoV-2 through SHERLOCK (Specific High Sensitivity Enzymatic Reporter UnLOCKing) Optimization, results within 1 hour, with sensitivity and specificity comparable to RT-qPCR and less than 5 per test [69]), OPTIMA-dx (a sensitive, robust, rapid, one-pot assay [70]), and DNA aptamer-conjugated graphene field-effect transistor (GFET) biosensor platform (label-free, results within 20 minutes, conducted with an ultrasensitive handheld wireless readout device [71]). Traveler screening and wastewater surveillance may facilitate the early detection of outbreaks and would likely reduce the amount of population-level testing required. Another important finding is the marginal effects between the testing interval and the benefit of a reduction in epidemic duration. Shortening the testing interval can significantly reduce the epidemic duration. However, this benefit is diminished at a 1-day testing interval. Previous studies showed that high percentage of contacts successfully traced is needed to control the outbreaks with historical variant [72,73]. Population-level testing (essentially another form of contact tracing) was used to compensate for the low percentage of contacts successfully traced (usually about 17%) in practice.

The use of real-time human mobility data presents an important opportunity to understand the dynamics and control of SARS-CoV-2 in a large country with modern transport systems within a densely populated setting. To quantify the potential severity of the Omicron outbreak, we used a counterfactual assumption that between-city travel restrictions would not be

implemented. Our results demonstrate that the effectiveness of travel restrictions depends upon both the timing of implementation and the specific variant. With timely travel restrictions between cities, the number of cities with outbreaks can be significantly reduced. Owing to the economic and social stresses imposed by this type of intervention, trade-offs between economic and public health objectives should be considered.

With the age-stratified metapopulation model incorporating population-level testing and contact tracing, the COVID-19 burden was also evaluated. Due to mass vaccination (especially in the ≥ 60 age group with 86% vaccine coverage by August 2022 in China), the hospital admissions and ICU admissions would be largely reduced. However, the disease burden would still overwhelm the health care system for respiratory illness without the testing. The underlying health conditions would increase the requirements for hospital and ICU beds. After calibrating the risk ratios and the prevalence of underlying health conditions, the 40–60 and ≥ 60 age groups would contribute to most extra hospital admission and ICU admission respectively, if the least stringent control strategy were employed. Among the underlying health conditions, obesity would contribute to most extra hospital admissions, while the hypertension could contribute to most extra ICU admissions. Interestingly, for 0–19 age group, obesity is expected to account for most extra hospital admissions. This is due to the relatively high prevalence of obesity (2.3%) in the young population and high hospitalization rate. More attention should be given to children and adolescents in regions with an increasing prevalence of obesity. We note that these estimations are based on the least-stringent control strategy. In our analysis, the independence among different underlying conditions is assumed. The impacts of multiple comorbid conditions for the same individuals on COVID-19 burden should be investigated, particularly in regions with an ageing population. Due to the scarcity of data, we also assumed that the age distribution of the prevalence of underlying health conditions is consistent between cities and country. The age-adjusted odds ratios (OR) for hospitalization and ICU admission for 8 types of underlying conditions were collected from multiple sources. Incomparability may exist among them. In addition, the hospitalization and ICU admission rate should also be calibrated to account for the underlying health conditions in a detailed way in the future.

There are limitations to this study. Under-reporting may have existed during the initial wave of COVID-19 in 2020 in China. Although different detection rates for symptomatic individuals were modeled, regional variations might not have been fully captured during that period. Additionally, human mobility is often influenced by holidays and other factors, which could impact the spread of the virus. While a typical outbreak scenario was simulated in the study, it is essential to acknowledge that real-world situations might be more complex and dynamic. Future work could focus on the changing epidemiological parameters of new variants [58]. Model calibration should be performed if vaccine effectiveness against infection with emerging variants is maintained, especially for the difference between breakthrough infections in vaccinated populations and waning vaccine effectiveness.

To conclude, we found that the epidemic duration of COVID-19 in China over the past 2 years was reduced by population-level testing. Marginal effects between the testing interval and the reduction in epidemic duration was observed. The control strategy with frequent population-wide testing would keep the COVID-19 burden under a manageable scale in China. The population-level testing might balance disease control and the harm to health, economies, and societies caused by travel restrictions between cities. We hope that the lessons learned from the public health measures in China may help to inform the health preparedness of COVID-19 pandemic, especially considering the unpredictable evolution of SARS-CoV-2 and the high prevalence of underlying conditions.

Methods

Epidemiological data

We collected daily official case reports from the health commission websites in 34 provincial-level administrative units and 366 city-level units [31]. Demographic data for each city were collected from the China City Statistical Yearbook 2019 (<http://olap.epsnet.com.cn/>).

Human mobility data

Human movement in China can be observed directly using mobile phone data with Baidu location-based services. We obtained both the recorded movements and relative volume of inflows, outflows, and internal movement among cities ($n = 366$) from the migration flows database (<http://qianxi.baidu.com/>) from 1 January 2019 to 1 April 2020. We considered the averaged between-city travel flow in 2019 as the flow at baseline and constructed a flow network across 366 cities in China to simulate SARS-CoV-2 transmission across Chinese cities. The travel flow during the first COVID-19 wave in 2020 was used to evaluate the effectiveness of initial version of public health measures.

Metapopulation models

To evaluate the effectiveness of the public health measures in China and incorporate variations in nonpharmaceutical interventions (NPIs), we developed three metapopulation models with increasing complexity. We first introduced the baseline metapopulation model to set up the context of modelling. Then, we extended the baseline model to account for social distancing to evaluate NPIs during the first epidemic wave and the Omicron-like wave in China. Finally, we developed a stochastic age-stratified metapopulation model that included population-level testing and contact tracing based on previous well-established models [74,75] to illustrate the effectiveness of the control strategy in a highly transmissible variant waves (e.g., Omicron BA.1) and quantitatively assess the number of infections and disease burden in each age group. The initial condition of the simulation is set as September 2022 since we performed the modeling analysis based on the vaccine coverage by August of 2022 in China. Please see the Supplementary Materials for more details.

Simulation scenarios

According to the fitted metapopulation model with social distancing and daily case reports from each city in the first wave of COVID-19, we simulated different scenarios by varying the strength of social distancing, travel restrictions between cities, vaccine coverage, and SARS-CoV-2 variants. The effectiveness of China's two-dose inactivated vaccines (BBIBP-CorV and CoronaVac) against infection was set to 40% for Omicron [76,77] and 59% for Wuhan-Hu-1 [78]. All scenarios used the same epidemic trajectories among cities. Using the age-stratified metapopulation model with population-level testing and contact tracing, we also performed sensitivity analysis for the testing interval and response lag for the variant with the basic reproduction number of 10 and 8. In this age-stratified model, the population-level testing at city level would be launched at response lag of 1, 2, 3, or 4 weeks after the first case was identified in the city. Contact tracing would be triggered for each infection irrespective of the presence of symptoms. The infections and the traced contacts would be isolated. Please refer to the Supplementary Materials.

The collection of risk ratios of hospitalization and ICU admission for COVID-19 cases with underlying conditions

We searched PubMed for articles reporting the odds ratios of hospitalization and ICU admission for COVID-19 cases with underlying health conditions. The search terms "COV" AND "underlying condition" AND "odds ratio" and "COV" AND "underlying condition" AND "OR" yielded 93 and 3,081 studies, respectively. As the odds ratios are highly dependent on age, the age-adjusted odds ratios are of interest and were collected. After screening, 12 studies remained, and they involved 14 types of underlying health conditions. For each underlying condition, the age-adjusted odds ratios for both hospitalization and ICU admission were needed. After this filter, 11 types of underlying health conditions remained. If multiple studies reported age-adjusted odds ratios, the highest one was selected.

The prevalence of the underlying health conditions in the Chinese population

For each underlying condition from the above risk ratio collection, we searched the reported prevalence in the Chinese population using PubMed and CNKI. In PubMed, the search terms were "China" AND "prevalence" AND name of the underlying condition AND province. The names of the underlying conditions were hypertension, diabetes, obesity, COPD, liver disease, kidney disease, asthma, cancer, cardiovascular disease, cardiac disorder and chronic respiratory disease. These searches generated 22,333 studies in total. For CNKI, the search terms were the same but in Chinese. This search yielded 3,821 studies. After screening the search results from PubMed and CNKI, most studies were found to be irrelevant. The studies reporting age-specific or province-specific prevalence with the latest publication date were selected. Finally, the prevalence for 8 types of underlying health conditions was collected. The age-adjusted risk ratio and the prevalence are shown in [Table 1](#).

The calculation of extra COVID-19 burden due to the underlying conditions

To evaluate the disease burden of the Omicron variant, the age-specific number of hospitalizations, and ICU admissions were measured quantitatively based on age-specific hospitalization and ICU admission rates ([S8 Table](#)). Previous studies suggested that individuals with underlying health conditions have higher risks of hospitalization and ICU admission. We first calculated the number of hospitalizations and ICU admissions as baseline by assuming all individuals were healthy (i.e., without underlying health conditions), and then calculated the number of hospitalizations and ICU admissions considering underlying health conditions across age groups. Finally, we used the difference between them as an extra disease burden due to underlying health conditions. The number of cases in each age group was derived from the age-stratified metapopulation model with population-level testing and contact tracing. Please see the Supplementary Materials for more details.

Supporting information

S1 Text. Supplementary text.
(DOCX)

S1 Fig. Heterogeneities in population distribution, intra-city movement reduction, movement inflow reduction, movement outflow reduction, before and after the travel restriction among Chinese cities during the first wave. The shading from light to dark represents the value from low to high. The base layer of the map is provided by GADM (File link: <https://>

gadm.org/download_country.html; License information: <https://gadm.org/license.html>).
(DOCX)

S2 Fig. Travel movements in China before and after the travel restriction. (A) Movement inflows in 2019 and 2020, averaged across 366 Chinese cities. The median (solid line) and interquartile range (shading) of values among cities are shown. The vertical dotted line represents the beginning of the Wuhan lockdown on 23rd January 2020. (B) Intra-city movements in China before and after travel restriction during the SARS-CoV-2 pandemic between January 1 and March 6, 2020. Line shade indicates the average number of daily travel movements (>300 are shown) for each pair of location. Point size represents the volume of travel inflow.
(DOCX)

S3 Fig. Travel movements and transmission pattern of the first SARS-CoV-2 wave in China. (A) Travel matrices before and after travel restriction. Lower-triangular values represent travel movements from city i to city j , and upper-triangular values from city j to city i . The shading from light to dark represents the volume of travel movements between pairs of cities from low to high. Black box represents the travel movements between cities within a province. The upper panel represents the total movements for each city, inflow (red) and outflow (blue). (B) Correlation of time series of reported cases between cities in the first wave of China. Cities are categorized by province and ranked from North (top) to South (bottom).
(DOCX)

S4 Fig. Pairwise correlation in daily COVID-19 cases between cities during the first wave in China. (A) Each point represents a pair of cities. Synchrony of the epidemics in the two cities is measured by the correlation between the number of cases reported in two cities on each day, using a spatial non-parametric correlation function (black line = estimated curve, dark grey area 95% confidence band). The synchrony declines with increasing geographical distance. (B) Pairs of cities are ranked according to the level of travel movements between them (from low to high). The city pairs are then classified into ten categories corresponding to quantiles of the rank. Box and whisker plots show distribution of epidemic synchrony scores for cities in each of the ten categories; The first box represents the correlation among Q1-Q1 pairs, the second is among Q1-Q2 pairs, up to the final bar which is among Q4-Q4 pairs. Pairs of cities with more travel movements have more synchronized epidemics.
(DOCX)

S5 Fig. Fits of the meta-population model with the social distancing on transmission rate during the first wave in China. Correlation between the number of cases reported in each city and model fitting by March 6, 2020. Circle size is proportional to the correlation coefficient between time series of reported cases and model prediction for each city.
(DOCX)

S6 Fig. Fits of meta-population model with the social distancing on transmission rate to time series of reported cases from cities during the first wave (city with more than 50 cases are shown). The numbers of confirmed cases reported (points) and estimated (lines) each day in each city. Grey areas correspond to pointwise 95% prediction envelopes.
(DOCX)

S7 Fig. Effectiveness of public health measures without population-level testing during Wuhan-Hu-1 and Omicron waves in China. (A) Predicted dependence of the average epidemic duration across all cities on travel restrictions between cities (from 100% strict restriction to 0% no restriction) and social distancing (a set of measures aiming at reduction of transmission rate, e.g., mask wearing, from strong [100%] to weak [0%]) for Wuhan-Hu-1

variant in the absence of vaccination. The estimated intensity of social distancing on reduction of transmission rate during the first wave in 2020 in China is indicated by the red cross. The fitting performance for the first wave can be found in S5 and S6 Figs. The simulation is based on the specific NPIs implemented during the first wave in 2020, except the strength of travel restrictions between cities. (B) Same as in (A) but for Omicron variant. (C) Predicted dependence of average epidemic duration across all Chinese cities on vaccine coverage and social distancing for the Omicron variant. The simulation is based on the specific NPIs implemented during the first wave in 2020. In (A) to (C), the Zero-COVID line (i.e., controlling the outbreak within 76 days) is shown as a dashed white line and solid line for Wuhan-Hu-1 and Omicron variants, respectively (see Methods). Note that the darker color with longer duration indicates that the whole population was infected, and the epidemic curve is either thin or flat. Effectiveness of China's inactivated vaccines (BBIBP-CorV and CoronaVac) against infection was set to 40% for Omicron and 59% for Wuhan-Hu-1. The full list of epidemiological parameters is given in S6 Table.

(DOCX)

S8 Fig. Number of COVID-19 cases under different response lags and testing intervals of population-level testing ($R_0 = 10$). Predicted number of COVID-19 cases across 366 cities in China under different testing intervals and response lags. The grey dot represents the median and the grey error bar represents the 95% CI based on the 100 simulations. The reduction of social distancing on transmission rate is set to 18% by considering the effect of only mask wearing against SARS-CoV-2 infection [8]. The vaccine coverage is set to 89% (consistent with 86% vaccine coverage in the ≥ 60 age group by August of 2022 in China) and the effectiveness of China's inactivated vaccine (BBIBP-CorV and CoronaVac) against infection was set to be 40% for Omicron [9].

(DOCX)

S9 Fig. Number of tests under different response lags and testing intervals of population-level testing ($R_0 = 10$). Predicted number of tests across 366 cities in China under different testing intervals and response lags. The grey dot represents the median and the grey error bar represents the 95% CI based on the 100 simulations. The reduction of social distancing on transmission rate is set to 18% by considering the effect of only mask wearing against SARS-CoV-2 infection [8]. The vaccine coverage is set to 89% (consistent with 86% vaccine coverage in the ≥ 60 age group by August of 2022 in China) and the effectiveness of China's inactivated vaccine (BBIBP-CorV and CoronaVac) against infection was set to be 40% for Omicron [9]. Note that when response lag is 3 weeks, cities with small population size may suffer from lockdown due to high proportion of population of cities were traced, and the outbreak is quickly contained, resulting in smaller number of tests.

(DOCX)

S10 Fig. Effectiveness of population-level testing in China under 4-day testing interval ($R_0 = 10$). Predicted epidemic duration and rounds of testing across 366 cities in China under different testing intervals and response lags when travel restrictions between cities is implemented with population-level testing. The grey dot represents the median and the grey error bar represents the 95% CI based on the 100 simulations. The dashed red line shows the duration of Wuhan's lockdown in 2020 (i.e., 76 days) as reference. The number of cities with local outbreaks is labeled below the violin plot. The reduction of social distancing on transmission rate is set to 18% by considering the effect of only mask wearing against SARS-CoV-2 infection [8]. The vaccine coverage is set to 89% (consistent with 86% vaccine coverage in the ≥ 60 age group by August of 2022 in China) and the effectiveness of China's inactivated vaccine

(BBIBP-CorV and CoronaVac) against infection was set to be 40% for Omicron [9].
(DOCX)

S11 Fig. Effectiveness of population-level testing combined with travel restrictions between cities in China during Omicron-like variant wave ($R_0 = 10$). Predicted epidemic duration and rounds of testing across 366 cities in China under different testing intervals and response lags when travel restrictions between cities is implemented with population-level testing. The grey dot represents the median and the grey error bar represents the 95% CI based on the 100 simulations. The dashed red line shows the duration of Wuhan's lockdown in 2020 (i.e., 76 days) as reference. The number of cities with local outbreaks is labeled below the violin plot. The reduction of social distancing on transmission rate is set to 18% by considering the effect of only mask wearing against SARS-CoV-2 infection [8]. The vaccine coverage is set to 89% (consistent with 86% vaccine coverage in the ≥ 60 age group by August of 2022 in China) and the effectiveness of China's inactivated vaccine (BBIBP-CorV and CoronaVac) against infection was set to be 40% for Omicron [9].
(DOCX)

S12 Fig. Effectiveness of population-level testing in China during Omicron-like variant wave when $R_0 = 8$. Predicted epidemic duration and rounds of testing across 366 cities in China under different testing intervals and response lags when travel restrictions between cities is implemented with population-level testing. The grey dot represents the median and the grey error bar represents the 95% CI based on the 100 simulations. The dashed red line shows the duration of Wuhan's lockdown in 2020 (i.e., 76 days) as reference. The number of cities with local outbreaks is labeled below the violin plot. The reduction of social distancing on transmission rate is set to 18% by considering the effect of only mask wearing against SARS-CoV-2 infection [8]. The vaccine coverage is set to 89% (consistent with 86% vaccine coverage in the ≥ 60 age group by August of 2022 in China) and the effectiveness of China's inactivated vaccine (BBIBP-CorV and CoronaVac) against infection was set to be 40% for Omicron [9].
(DOCX)

S13 Fig. Effectiveness of population-level testing in China during Omicron wave ($R_0 = 10$) when $rI = 2$. Predicted epidemic duration and rounds of testing across 366 cities in China under different testing intervals and response lags when travel restrictions between cities is implemented with population-level testing. The grey dot represents the median and the grey error bar represents the 95% CI based on the 100 simulations. The dashed red line shows the duration of Wuhan's lockdown in 2020 (i.e., 76 days) as reference. The number of cities with local outbreaks is labeled below the violin plot. The reduction of social distancing on transmission rate is set to 18% by considering the effect of only mask wearing against SARS-CoV-2 infection. The vaccine coverage is set to 89% (consistent with 86% vaccine coverage in the ≥ 60 age group by August of 2022 in China) and the effectiveness of China's inactivated vaccine (BBIBP-CorV and CoronaVac) against infection was set to be 40% for Omicron.
(DOCX)

S14 Fig. Comparison of epidemic duration and rounds of testing between two successive testing intervals without travel restrictions between cities ($R_0 = 10$). Response lag is set to 2 weeks. A negative value corresponds to benefits yielded for duration or rounds by speeding up testing (shorten testing interval), and a positive value corresponds to potential loss for duration or rounds by speeding up testing. The red and blue dots represent median and grey error bar represents the 95% CI based on the 100 simulations. The reduction of social distancing on transmission rate is set to 18% by considering the effect of only mask wearing against SARS-CoV-2

infection [8]. The vaccine coverage is set to 89% (consistent with 86% vaccine coverage in the ≥ 60 age group by August of 2022 in China) and the effectiveness of China's inactivated vaccine (BBIBP-CorV and CoronaVac) against infection was set to be 40% for Omicron [9].

(DOCX)

S15 Fig. Comparison of epidemic duration and rounds of testing between two successive testing intervals when travel restrictions between cities is implemented ($R_0 = 10$). (A)

Response lag is set to 2 weeks. (B) Response lag is set to 3 weeks. A negative value corresponds to benefits yielded for duration or rounds by speeding up testing (shorten testing interval), and a positive value corresponds to potential loss for duration or rounds by speeding up testing. The red and blue dots represent median and grey error bar represents the 95% CI based on the 100 simulations. The reduction of social distancing on transmission rate is set to 18% by considering the effect of only mask wearing against SARS-CoV-2 infection [8]. The vaccine coverage is set to 89% (consistent with 86% vaccine coverage in the ≥ 60 age group by August of 2022 in China) and the effectiveness of China's inactivated vaccine (BBIBP-CorV and CoronaVac) against infection was set to be 40% for Omicron [9].

(DOCX)

S16 Fig. Potential impact of control strategy with long response lag on SARS-CoV-2 infections and daily life. (A)

The total SARS-CoV-2 infections for different age groups when testing interval is 3 days and response lag is 3 weeks. The dot represents the infections for an age group and a city. (B) Association between population size and proportion of isolated population across 366 cities in China when testing interval is 3 days and response lag is 3 weeks. The size and color of the circle represent the movement flow and the proportion of isolated population in a given city, respectively.

(DOCX)

S17 Fig. COVID-19 burden for Omicron-like variant ($R_0 = 10$) under 4-day testing interval. (A)

Daily required hospital beds for different age groups. (B) Daily required ICU beds for different age groups. The response lag is set to be 3 weeks. The grey error bar or shadow represents the 95% CI for 100 simulations. The red dashed line represents the total available hospital beds or ICU beds in China. The vaccine coverage for all age groups was set to be 89%, consistent with 86% vaccine coverage in the ≥ 60 age group by August of 2022 in China.

(DOCX)

S18 Fig. COVID-19 burden for Omicron-like variant ($R_0 = 10$) under the control strategy in China for optimistic scenario. (A)

Daily required hospital beds for different age groups. (B) Daily required ICU beds for different age groups. The control strategy was employed with a testing interval of 3 days and a response lag of 3 weeks (the effective reproduction number $R_e < 1$), which is the least stringent strategy aiming at suppressing SARS-CoV-2, as shown in Fig 2A. A strategy with a testing interval of 4 days and a response lag of 3 weeks would lead to the endemic of COVID-19 as shown in the grey dashed line with $R_e \approx 1$. The red dashed line represents the total available hospital beds or ICU beds in China. The grey solid line represents the peak number of required hospital beds or ICU beds during the pandemic without testing ($R_e > 1$). The grey error bar or shadow represents the 95% CI for 100 simulations. The vaccine coverage for all age groups was set to be 89%, consistent with 86% vaccine coverage in the ≥ 60 age group by August of 2022 in China. The effectiveness of China's inactivated vaccine (BBIBP-CorV and CoronaVac) against hospitalization and ICU admission were set to be 78.8% considering an optimistic scenario [10,11].

(DOCX)

S19 Fig. COVID-19 burden for Omicron-like variant ($R_0 = 10$) under the control strategy in China for pessimistic scenario. (A) Daily required hospital beds for different age groups. (B) Daily required ICU beds for different age groups. The control strategy was employed with a testing interval of 3 days and a response lag of 3 weeks (the effective reproduction number $R_e < 1$), which is the least stringent strategy aiming at suppressing SARS-CoV-2, as shown in Fig 2A. A strategy with a testing interval of 4 days and a response lag of 3 weeks would lead to the endemic of COVID-19 as shown in the grey dashed line with $R_e \approx 1$. The red dashed line represents the total available hospital beds or ICU beds in China. The grey solid line represents the peak number of required hospital beds or ICU beds during the pandemic without testing ($R_e > 1$). The grey error bar or shadow represents the 95% CI for 100 simulations. The vaccine coverage for all age groups was set to be 89%, consistent with 86% vaccine coverage in the ≥ 60 age group by August of 2022 in China. The effectiveness of China's inactivated vaccine (BBIBP-CorV and CoronaVac) against hospitalization and ICU admission were set to be 62.6% considering an pessimistic scenario [10,11].

(DOCX)

S20 Fig. COVID-19 burden for Omicron-like variant ($R_0 = 10$) under the control strategy in China for Hong Kong-specific age-dependent hospitalization and ICU admission rates.

(A) Daily required hospital beds for different age groups. (B) Daily required ICU beds for different age groups. The control strategy was employed with a testing interval of 3 days and a response lag of 3 weeks (the effective reproduction number $R_e < 1$), which is the least stringent strategy aiming at suppressing SARS-CoV-2, as shown in Fig 2A. A strategy with a testing interval of 4 days and a response lag of 3 weeks would lead to the endemic of COVID-19 as shown in the grey dashed line with $R_e \approx 1$. The red dashed line represents the total available hospital beds or ICU beds in China. The grey dotted line represents the strategy with a testing interval of 4 days and a response lag of 3 weeks. The grey solid line represents the peak number of required hospital beds or ICU beds during the pandemic without testing ($R_e > 1$). The grey error bar or shadow represents the 95% CI for 100 simulations. The vaccine coverage for all age groups was set to be 89%, consistent with 86% vaccine coverage in the ≥ 60 age group by August of 2022 in China. The age-dependent hospitalization and ICU admission rates were set according to data from the fifth wave of COVID-19 in Hong Kong in early 2022 [12].

(DOCX)

S21 Fig. COVID-19 burden for Omicron-like variant ($R_0 = 10$) under the control strategy in China for Shanghai-specific age-dependent ICU admission rates. Daily required ICU beds for different age groups. The control strategy was employed with a testing interval of 3 days and a response lag of 3 weeks (the effective reproduction number $R_e < 1$), which is the least stringent strategy aiming at suppressing SARS-CoV-2, as shown in Fig 2A. A strategy with a testing interval of 4 days and a response lag of 3 weeks would lead to the endemic of COVID-19 as shown in the grey dashed line with $R_e \approx 1$. The red dashed line represents the total available ICU beds in China. The grey dotted line represents the strategy with a testing interval of 4 days and a response lag of 3 weeks. The grey solid line represents the peak number of required ICU beds during the pandemic without testing ($R_e > 1$). The grey error bar or shadow represents the 95% CI for 100 simulations. The vaccine coverage for all age groups was set to be 89%, consistent with 86% vaccine coverage in the ≥ 60 age group by August of 2022 in China. The age-dependent ICU admission rates were set according to data from the Omicron wave of COVID-19 in Shanghai in early 2022 [13]. Due to the lack of hospitalization data in Omicron wave of COVID-19 in Shanghai, only the ICU burden of COVID-19 for the Omicron variant was evaluated under this scenario.

(DOCX)

S22 Fig. Potential impact of control strategy with short response lag on SARS-CoV-2 infections and daily life. (A) The total SARS-CoV-2 infections for different age groups when testing interval is 3 days and response lag is 2 weeks. The dot represents the infections for an age group and a city. (B) Association between population size and proportion of isolated population across 366 cities in China when testing interval is 3 days and response lag is 2 weeks. The size and color of the circle represent the movement flow and the proportion of isolated population in a given city, respectively.

(DOCX)

S23 Fig. The disease burden for Omicron-like variant ($R_0 = 10$) outbreak without considering the underlying health conditions. (A) The number of hospitalizations and (B) ICU admissions when the least stringent control strategy is employed. We considered all the infected individuals were healthy in the baseline scenario. The grey error bar or shadow represents the 95% CI for 100 simulations.

(DOCX)

S1 Table. The outbreaks controlled by public health measures in China.

(DOCX)

S2 Table. Estimated parameters values in the first wave of 2020 in China.

(DOCX)

S3 Table. The significance of reduction in epidemic duration and rounds of testing by shorter response lag (weeks) from the t -test.

(DOCX)

S4 Table. The significance of reduction in epidemic duration and rounds of testing by shorter testing interval from the t -test.

(DOCX)

S5 Table. The number of cities with the peak number of isolated individuals reaching the population size during the outbreak under different combinations of testing intervals and response lags. The isolated individuals include the individuals exposed to the SARS-CoV-2 and the infected individuals.

(DOCX)

S6 Table. Baseline model parameter values.

(DOCX)

S7 Table. Population-level testing and contact tracing model parameter values.

(DOCX)

S8 Table. Age-dependent hospitalization and ICU admission rates for symptomatic Omicron- infection in vaccinated and unvaccinated individuals. The effectiveness of China's inactivated vaccine (BBIBP-CorV and CoronaVac) against hospitalization and ICU admission were set to be 70% for Omicron for all age groups [11].

(DOCX)

Acknowledgments

We thank the thousands of Centers for Disease Control (CDC) staff and local health workers in China who collected data and continue to work to contain COVID-19 in China and elsewhere.

Author Contributions

Conceptualization: Zengmiao Wang.

Data curation: Lin Wang, Bingying Li, Yonghong Liu, Yuxi Ge.

Formal analysis: Zengmiao Wang, Peiyi Wu, Ruixue Wang.

Methodology: Zengmiao Wang, Peiyi Wu.

Visualization: Zengmiao Wang, Peiyi Wu, Ruixue Wang.

Writing – original draft: Zengmiao Wang.

Writing – review & editing: Zengmiao Wang, Peiyi Wu, Lin Wang, Ligui Wang, Hua Tan, Chieh-Hsi Wu, Marko Laine, Henrik Salje, Hongbin Song.

References

1. Chen J-M, Chen Y-Q. China can prepare to end its zero-COVID policy. *Nat Med.* 2022; 28: 1104–1105. <https://doi.org/10.1038/s41591-022-01794-3> PMID: 35383312
2. Li Z, Liu F, Cui J, Peng Z, Chang Z, Lai S, et al. Comprehensive large-scale nucleic acid-testing strategies support China's sustained containment of COVID-19. *Nat Med.* 2021; 27: 740–742. <https://doi.org/10.1038/s41591-021-01308-7> PMID: 33859409
3. Burki T. Hong Kong's fifth COVID-19 wave—the worst yet. *Lancet Infect Dis.* 2022; 22: 455–456. [https://doi.org/10.1016/S1473-3099\(22\)00167-0](https://doi.org/10.1016/S1473-3099(22)00167-0) PMID: 35338874
4. Zhang X, Zhang W, Chen S. Shanghai's life-saving efforts against the current omicron wave of the COVID-19 pandemic. *Lancet.* 2022; 399: 2011–2012. [https://doi.org/10.1016/S0140-6736\(22\)00838-8](https://doi.org/10.1016/S0140-6736(22)00838-8) PMID: 35533708
5. Fan X, Lu S, Bai L, Liu H, Fu J, Jin X, et al. Preliminary Study of the Protectiveness of Vaccination Against the COVID-19 in the Outbreak of VOC Omicron BA.2 —Jilin City, Jilin Province, China, March 3–April 12, 2022. *China CDC Wkly.* 2022; 4: 377–380. <https://doi.org/10.46234/ccdcw2022.081> PMID: 35686205
6. China Focus: China releases measures to optimize COVID-19 response-Xinhua. [cited 29 Dec 2022]. <https://english.news.cn/20221111/d4399114a082438eaac32d08a02bf58d/c.html>
7. China Focus: COVID-19 response further optimized with 10 new measures-Xinhua. [cited 29 Dec 2022]. <https://english.news.cn/20221207/ca014c043bf24728b8dcbc0198565fdf/c.html>
8. China enters new phase of COVID response-Xinhua. [cited 19 Jan 2023]. <https://english.news.cn/20230109/1521678fe36247b3959ac5bab8e496a9/c.html>
9. Leung K, Lau EHY, Wong CKH, Leung GM, Wu JT. Estimating the transmission dynamics of SARS-CoV-2 Omicron BF.7 in Beijing after adjustment of the zero-COVID policy in November-December 2022. *Nat Med.* 2023; 29: 579–582. <https://doi.org/10.1038/s41591-023-02212-y> PMID: 36638825
10. Pan Y, Wang L, Feng Z, Xu H, Li F, Shen Y, et al. Characterisation of SARS-CoV-2 variants in Beijing during 2022: an epidemiological and phylogenetic analysis. *Lancet.* 2023; 401: 664–672. [https://doi.org/10.1016/S0140-6736\(23\)00129-0](https://doi.org/10.1016/S0140-6736(23)00129-0) PMID: 36773619
11. Lenharo M. WHO declares end to COVID-19's emergency phase. *Nature.* 2023 [cited 24 May 2023]. <https://doi.org/10.1038/d41586-023-01559-z> PMID: 37147368
12. European Centre for Disease Prevention and Control. Population-wide testing of SARS-CoV-2: country experiences and potential approaches in the EU/EEA and the United Kingdom. 2020 [cited 4 Jan 2023]. <https://www.ecdc.europa.eu/sites/default/files/documents/covid-19-population-wide-testing-country-experiences.pdf>
13. Press Conference of the Joint Prevention and Control Mechanism of the State Council. 2022. <http://www.gov.cn/xinwen/gwylflkjz211/index.htm>
14. Hellewell J, Russell TW, Beale R, Kelly G, Houlihan C, Nastouli E, et al. Estimating the effectiveness of routine asymptomatic PCR testing at different frequencies for the detection of SARS-CoV-2 infections. *BMC Med.* 2021; 19: 106. <https://doi.org/10.1186/s12916-021-01982-x> PMID: 33902581
15. Aleta A, Martín-Corral D, Pastore y Piontti A, Ajelli M, Litvinova M, Chinazzi M, et al. Modelling the impact of testing, contact tracing and household quarantine on second waves of COVID-19. *Nat Hum Behav.* 2020; 4: 964–971. <https://doi.org/10.1038/s41562-020-0931-9> PMID: 32759985

16. Wells CR, Townsend JP, Pandey A, Moghadas SM, Krieger G, Singer B, et al. Optimal COVID-19 quarantine and testing strategies. *Nat Commun.* 2021; 12: 1–9. <https://doi.org/10.1038/s41467-020-20742-8> PMID: 33414470
17. Bastani H, Drakopoulos K, Gupta V, Vlachogiannis I, Hadjicristodoulou C, Lagiou P, et al. Efficient and targeted COVID-19 border testing via reinforcement learning. *Nature.* 2021; 599: 108–113. <https://doi.org/10.1038/s41586-021-04014-z> PMID: 34551425
18. Long QX, Tang XJ, Shi QL, Li Q, Deng HJ, Yuan J, et al. Clinical and immunological assessment of asymptomatic SARS-CoV-2 infections. *Nat Med.* 2020; 26: 1200–1204. <https://doi.org/10.1038/s41591-020-0965-6> PMID: 32555424
19. Li R, Pei S, Chen B, Song Y, Zhang T, Yang W, et al. Substantial undocumented infection facilitates the rapid dissemination of novel coronavirus (SARS-CoV-2). *Science.* 2020; 368: 489–493. <https://doi.org/10.1126/science.abb3221> PMID: 32179701
20. Holt E. Slovakia to test all adults for SARS-CoV-2. *Lancet.* 2020; 396: 1386–1387. [https://doi.org/10.1016/S0140-6736\(20\)32261-3](https://doi.org/10.1016/S0140-6736(20)32261-3) PMID: 33129382
21. Pavelka M, Van-Zandvoort K, Abbott S, Sherratt K, Majdan M, Analýz IZ, et al. The impact of population-wide rapid antigen testing on SARS-CoV-2 prevalence in Slovakia. *Science.* 2021; 372: 635–641. <https://doi.org/10.1126/science.abc9648> PMID: 33758017
22. Frnda J, Durica M. On Pilot Massive COVID-19 Testing by Antigen Tests in Europe. Case Study: Slovakia. *Infect Dis Rep.* 2021; 13: 45–57. <https://doi.org/10.3390/idr13010007> PMID: 33430283
23. Elliott J, Whitaker M, Bodinier B, Eales O, Riley S, Ward H, et al. Predictive symptoms for COVID-19 in the community: REACT-1 study of over 1 million people. *PLoS Med.* 2021; 18: e1003777. <https://doi.org/10.1371/journal.pmed.1003777> PMID: 34582457
24. Elliott P, Eales O, Steyn N, Tang D, Bodinier B, Wang H, et al. Twin peaks: The Omicron SARS-CoV-2 BA.1 and BA.2 epidemics in England. *Science.* 2022; 376: eabq4411. <https://doi.org/10.1126/SCIENCE.ABQ4411> PMID: 35608440
25. Ranoa DRE, Holland RL, Alnaji FG, Green KJ, Wang L, Fredrickson RL, et al. Mitigation of SARS-CoV-2 transmission at a large public university. *Nat Commun.* 2022; 13: 3207. <https://doi.org/10.1038/s41467-022-30833-3> PMID: 35680861
26. Dewald F, Suárez I, Johnen R, Grossbach J, Moran-Tovar R, Steger G, et al. Effective high-throughput RT-qPCR screening for SARS-CoV-2 infections in children. *Nat Commun.* 2022; 13: 3640. <https://doi.org/10.1038/s41467-022-30664-2> PMID: 35752615
27. Diederichs M, van Ewijk R, Isphording IE, Pestel N. Schools under mandatory testing can mitigate the spread of SARS-CoV-2. *Proc Natl Acad Sci U S A.* 2022; 119: e2201724119. <https://doi.org/10.1073/pnas.2201724119> PMID: 35733261
28. Yuan P, Tan Y, Yang L, Aruffo E, Ogden NH, Yang G, et al. Assessing the mechanism of citywide test-trace-isolate Zero-COVID policy and exit strategy of COVID-19 pandemic. *Infect Dis poverty.* 2022; 11: 104. <https://doi.org/10.1186/s40249-022-01030-7> PMID: 36192815
29. Kraemer MUG, Yang CH, Gutierrez B, Wu CH, Klein B, Pigott DM, et al. The effect of human mobility and control measures on the COVID-19 epidemic in China. *Science.* 2020; 368: 493–497. <https://doi.org/10.1126/science.abb4218> PMID: 32213647
30. Lai S, Ruktanonchai NW, Zhou L, Prosper O, Luo W, Floyd JR, et al. Effect of non-pharmaceutical interventions to contain COVID-19 in China. *Nature.* 2020; 585: 410–413. <https://doi.org/10.1038/s41586-020-2293-x> PMID: 32365354
31. Tian H, Liu Y, Li Y, Wu CH, Chen B, Kraemer MUG, et al. An investigation of transmission control measures during the first 50 days of the COVID-19 epidemic in China. *Science.* 2020; 368: 638–642. <https://doi.org/10.1126/science.abb6105> PMID: 32234804
32. Ruktanonchai NW, Floyd JR, Lai S, Ruktanonchai CW, Sadilek A, Rente-Lourenco P, et al. Assessing the impact of coordinated COVID-19 exit strategies across Europe. *Science.* 2020; 369: 1465–1470. <https://doi.org/10.1126/science.abc5096> PMID: 32680881
33. Chinazzi M, Davis JT, Ajelli M, Gioannini C, Litvinova M, Merler S, et al. The effect of travel restrictions on the spread of the 2019 novel coronavirus (COVID-19) outbreak. *Science.* 2020; 368: 395–400. <https://doi.org/10.1126/science.aba9757> PMID: 32144116
34. Lai S, Ruktanonchai NW, Carioli A, Ruktanonchai CW, Floyd JR, Prosper O, et al. Assessing the Effect of Global Travel and Contact Restrictions on Mitigating the COVID-19 Pandemic. *Engineering.* 2021; 7: 914–923. <https://doi.org/10.1016/j.eng.2021.03.017> PMID: 33972889
35. Mendelson M, Venter F, Moshabela M, Gray G, Blumberg L, de Oliveira T, et al. The political theatre of the UK's travel ban on South Africa. *Lancet.* 2021; 398: 2211–2213. [https://doi.org/10.1016/S0140-6736\(21\)02752-5](https://doi.org/10.1016/S0140-6736(21)02752-5) PMID: 34871546

36. Kucharski AJ, Jit M, Logan JG, Cotten M, Clifford S, Quilty BJ, et al. Travel measures in the SARS-CoV-2 variant era need clear objectives. *Lancet*. 2022; 399: 1367–1369. [https://doi.org/10.1016/S0140-6736\(22\)00366-X](https://doi.org/10.1016/S0140-6736(22)00366-X) PMID: 35247312
37. Pierce M, Hope H, Ford T, Hatch S, Hotopf M, John A, et al. Mental health before and during the COVID-19 pandemic: a longitudinal probability sample survey of the U.K. population. *Lancet Psychiat*. 2020; 7: 883–892. [https://doi.org/10.1016/S2215-0366\(20\)30308-4](https://doi.org/10.1016/S2215-0366(20)30308-4) PMID: 32707037
38. Elmer T, Mepham K, Stadtfeld C. Students under lockdown: Comparisons of students' social networks and mental health before and during the COVID-19 crisis in Switzerland. *PLoS One*. 2020; 15: e0236337. <https://doi.org/10.1371/journal.pone.0236337> PMID: 32702065
39. Giuntella O, Hyde K, Saccardo S, Sadoff S. Lifestyle and mental health disruptions during COVID-19. *Proc Natl Acad Sci U S A*. 2021; 118: e2016632118. <https://doi.org/10.1073/pnas.2016632118> PMID: 33571107
40. Aragona M, Barbato A, Cavani A, Costanzo G, Mirisola C. Negative impacts of COVID-19 lockdown on mental health service access and follow-up adherence for immigrants and individuals in socio-economic difficulties. *Public Health*. 2020; 186: 52–56. <https://doi.org/10.1016/j.puhe.2020.06.055> PMID: 32771661
41. Brown A, Flint SW, Kalea AZ, O'Kane M, Williams S, Batterham RL. Negative impact of the first COVID-19 lockdown upon health-related behaviours and psychological wellbeing in people living with severe and complex obesity in the UK. *EClinicalMedicine*. 2021; 34: 100796. <https://doi.org/10.1016/j.eclinm.2021.100796> PMID: 33754138
42. de la Rosa PA, Cowden RG, de Filippis R, Jerotic S, Nahidi M, Ori D, et al. Associations of lockdown stringency and duration with Google searches for mental health terms during the COVID-19 pandemic: A nine-country study. *J Psychiatr Res*. 2022; 150: 237–245. <https://doi.org/10.1016/j.jpsychires.2022.03.026> PMID: 35398667
43. Brooks SK, Webster RK, Smith LE, Woodland L, Wessely S, Greenberg N, et al. The psychological impact of quarantine and how to reduce it: rapid review of the evidence. *Lancet*. 2020; 395: 912–920. [https://doi.org/10.1016/S0140-6736\(20\)30460-8](https://doi.org/10.1016/S0140-6736(20)30460-8) PMID: 32112714
44. Mallapaty S. Where did Omicron come from? Three key theories. *Nature*. 2022; 602: 26–28. <https://doi.org/10.1038/d41586-022-00215-2> PMID: 35091701
45. Tegally H, Moir M, Everatt J, Giovanetti M, Scheepers C, Wilkinson E, et al. Emergence of SARS-CoV-2 Omicron lineages BA.4 and BA.5 in South Africa. *Nat Med*. 2022; 28: 1785–1790. <https://doi.org/10.1038/s41591-022-01911-2> PMID: 35760080
46. Cao Y, Yisimayi A, Jian F, Song W, Xiao T, Wang L, et al. BA.2.12.1, BA.4 and BA.5 escape antibodies elicited by Omicron infection. *Nature*. 2022; 608: 593–602. <https://doi.org/10.1038/s41586-022-04980-y> PMID: 35714668
47. Khan K, Karim F, Ganga Y, Bernstein M, Jule Z, Reedoy K, et al. Omicron BA.4/BA.5 escape neutralizing immunity elicited by BA.1 infection. *Nat Commun*. 2022; 13: 4686. <https://doi.org/10.1038/s41467-022-32396-9> PMID: 35948557
48. Liang S, Jiang T, Jiao Z, Zhou Z. A model simulation of a containment of the SARS-CoV-2 Omicron variant in Beijing, China. *Intell Med*. 2022; 3: 10–15. <https://doi.org/10.1016/J.IMED.2022.10.005> PMID: 36438437
49. Wang Y, Sun K, Feng Z, Yi L, Wu Y, Liu H, et al. Assessing the feasibility of sustaining SARS-CoV-2 local containment in China in the era of highly transmissible variants. *BMC Med*. 2022; 20: 442. <https://doi.org/10.1186/s12916-022-02640-6> PMID: 36380354
50. Cai J, Deng X, Yang J, Sun K, Liu H, Chen Z, et al. Modeling transmission of SARS-CoV-2 Omicron in China. *Nat Med*. 2022; 28: 1468–1475. <https://doi.org/10.1038/s41591-022-01855-7> PMID: 35537471
51. Wang Z, Wang R, Wu P, Li B, Li Y, Liu Y, et al. Optimization of Population-Level Testing, Contact Tracing, and Isolation in Emerging COVID-19 Outbreaks: a Mathematical Modeling Study—Tonghua City and Beijing Municipality, China, 2021–2022. *China CDC Wkly*. 2023; 5: 82–89. <https://doi.org/10.46234/ccdcw2023.016> PMID: 36777897
52. National Health Commission of China. *China Health Statistics Yearbook 2021*. 2021.
53. Transcript of the press conference of the Joint Prevention and Control Mechanism of the State Council on December 9, 2022. [cited 19 Jan 2023]. <http://www.nhc.gov.cn/cms-search/xxgk/getManuscriptXxgk.htm?id=d9f06b80eaaf4e37bf1023e9bb89d711>
54. Abbott S, Sherratt K, Gerstung M, Funk S. Estimation of the test to test distribution as a proxy for generation interval distribution for the Omicron variant in England. medRxiv. 2022 [cited 21 Jan 2023]. <https://doi.org/10.1101/2022.01.08.22268920>
55. Kim D, Ali ST, Kim S, Jo J, Lim JS, Lee S, et al. Estimation of Serial Interval and Reproduction Number to Quantify the Transmissibility of SARS-CoV-2 Omicron Variant in South Korea. *Viruses*. 2022; 14: 533. <https://doi.org/10.3390/v14030533> PMID: 35336939

56. Ito K, Piantham C, Nishiura H. Estimating relative generation times and reproduction numbers of Omicron BA.1 and BA.2 with respect to Delta variant in Denmark. *Math Biosci Eng.* 2022; 19: 9005–9017. <https://doi.org/10.3934/mbe.2022418> PMID: 35942746
57. Ali ST, Wang L, Lau EHY, Xu XK, Du Z, Wu Y, et al. Serial interval of SARS-CoV-2 was shortened over time by nonpharmaceutical interventions. *Science.* 2020; 369: 1106–1109. <https://doi.org/10.1126/science.abc9004> PMID: 32694200
58. Kraemer MUG, Pybus OG, Fraser C, Cauchemez S, Rambaut A, Cowling BJ. Monitoring key epidemiological parameters of SARS-CoV-2 transmission. *Nat Med.* 2021; 27: 1854–1855. <https://doi.org/10.1038/s41591-021-01545-w> PMID: 34750555
59. Tindale LC, Stockdale JE, Coombe M, Garlock ES, Lau WYV, Saraswat M, et al. Evidence for transmission of COVID-19 prior to symptom onset. *Elife.* 2020; 9: 1–34. <https://doi.org/10.7554/eLife.57149> PMID: 32568070
60. Park SW, Sun K, Champredon D, Li M, Bolker BM, Earn DJD, et al. Forward-looking serial intervals correctly link epidemic growth to reproduction numbers. *Proc Natl Acad Sci U S A.* 2021; 118: e2011548118. <https://doi.org/10.1073/pnas.2011548118> PMID: 33361331
61. Stockdale JE, Susvitasari K, Tupper P, Sobkowiak B, Mulberry N, da Silva AG, et al. Genomic epidemiology offers high resolution estimates of serial intervals for COVID-19. *Nat Commun.* 2023; 14: 4830. <https://doi.org/10.1038/s41467-023-40544-y> PMID: 37563113
62. Wells CR, Pandey A, Moghadas SM, Singer BH, Krieger G, Heron RJL, et al. Comparative analyses of eighteen rapid antigen tests and RT-PCR for COVID-19 quarantine and surveillance-based isolation. *Commun Med.* 2022; 2: 84. <https://doi.org/10.1038/s43856-022-00147-y> PMID: 35822105
63. Larremore DB, Wilder B, Lester E, Shehata S, Burke JM, Hay JA, et al. Test sensitivity is secondary to frequency and turnaround time for COVID-19 screening. *Sci Adv.* 2021; 7: eabd5393. <https://doi.org/10.1126/sciadv.abd5393> PMID: 33219112
64. Mina MJ, Parker R, Larremore DB. Rethinking Covid-19 Test Sensitivity—A Strategy for Containment. *N Engl J Med.* 2020; 383: e120. <https://doi.org/10.1056/NEJMp2025631> PMID: 32997903
65. Mina MJ, Peto TE, García-Fiñana M, Semple MG, Buchan IE. Clarifying the evidence on SARS-CoV-2 antigen rapid tests in public health responses to COVID-19. *Lancet.* 2021; 397: 1425–1427. [https://doi.org/10.1016/S0140-6736\(21\)00425-6](https://doi.org/10.1016/S0140-6736(21)00425-6) PMID: 33609444
66. Chu VT, Schwartz NG, Donnelly MAP, Chuey MR, Soto R, Yousaf AR, et al. Comparison of Home Antigen Testing With RT-PCR and Viral Culture During the Course of SARS-CoV-2 Infection. *JAMA Intern Med.* 2022; 182: 701–709. <https://doi.org/10.1001/jamainternmed.2022.1827> PMID: 35486394
67. Cleary B, Hay JA, Blumenstiel B, Harden M, Cipicchio M, Bezney J, et al. Using viral load and epidemic dynamics to optimize pooled testing in resource-constrained settings. *Sci Transl Med.* 2021; 13: eabf1568. <https://doi.org/10.1126/scitranslmed.abf1568> PMID: 33619080
68. Barak N, Ben Ami R, Sido T, Perri A, Shtoyer A, Rivkin M, et al. Lessons from applied large-scale pooling of 133,816 SARS-CoV-2 RT-PCR tests. *Sci Transl Med.* 2021; 13: 2823. <https://doi.org/10.1126/scitranslmed.abf2823> PMID: 33619081
69. Casati B, Verdi JP, Hempelmann A, Kittel M, Klaebisch AG, Meister B, et al. Rapid, adaptable and sensitive Cas13-based COVID-19 diagnostics using ADESSO. *Nat Commun.* 2022; 13: 3308. <https://doi.org/10.1038/s41467-022-30862-y> PMID: 35676259
70. Mahas A, Marsic T, Lopez-Portillo Masson M, Wang Q, Aman R, Zheng C, et al. Characterization of a thermostable Cas13 enzyme for one-pot detection of SARS-CoV-2. *Proc Natl Acad Sci U S A.* 2022; 119: e2118260119. <https://doi.org/10.1073/pnas.2118260119> PMID: 35763567
71. Ban DK, Bodily T, Karkisaval AG, Dong Y, Natani S, Ramanathan A, et al. Rapid self-test of unprocessed viruses of SARS-CoV-2 and its variants in saliva by portable wireless graphene biosensor. *Proc Natl Acad Sci U S A.* 2022; 119: e2206521119. <https://doi.org/10.1073/pnas.2206521119> PMID: 35763566
72. Hellewell J, Abbott S, Gimma A, Bosse NI, Jarvis CI, Russell TW, et al. Feasibility of controlling COVID-19 outbreaks by isolation of cases and contacts. *Lancet Glob Heal.* 2020; 8: e488–e496. [https://doi.org/10.1016/S2214-109X\(20\)30074-7](https://doi.org/10.1016/S2214-109X(20)30074-7) PMID: 32119825
73. Kucharski AJ, Klepac P, Conlan AJK, Kissler SM, Tang ML, Fry H, et al. Effectiveness of isolation, testing, contact tracing, and physical distancing on reducing transmission of SARS-CoV-2 in different settings: a mathematical modelling study. *Lancet Infect Dis.* 2020; 20: 1151–1160. [https://doi.org/10.1016/S1473-3099\(20\)30457-6](https://doi.org/10.1016/S1473-3099(20)30457-6) PMID: 32559451
74. Ferretti L, Wymant C, Kendall M, Zhao L, Nurtay A, Abeler-Dörner L, et al. Quantifying SARS-CoV-2 transmission suggests epidemic control with digital contact tracing. *Science.* 2020; 368: eabb6936. <https://doi.org/10.1126/science.abb6936> PMID: 32234805
75. Klinkenberg D, Fraser C, Heesterbeek H. The effectiveness of contact tracing in emerging epidemics. *PLoS One.* 2006; 1: e12. <https://doi.org/10.1371/journal.pone.0000012> PMID: 17183638

76. Cerqueira-Silva T, Andrews JR, Boaventura VS, Ranzani OT, De V, Oliveira A, et al. Effectiveness of CoronaVac, ChAdOx1 nCoV-19, BNT162b2, and Ad26.COV2.S among individuals with previous SARS-CoV-2 infection in Brazil: a test-negative, case-control study. *Lancet Infect Dis.* 2022; 22: 791–801. [https://doi.org/10.1016/S1473-3099\(22\)00140-2](https://doi.org/10.1016/S1473-3099(22)00140-2) PMID: 35366959
77. Jara A, Undurraga EA, Zubizarreta JR, González C, Acevedo J, Pizarro A, et al. Effectiveness of CoronaVac in children 3–5 years of age during the SARS-CoV-2 Omicron outbreak in Chile. *Nat Med.* 2022; 28: 1377–1380. <https://doi.org/10.1038/s41591-022-01874-4> PMID: 35605637
78. Li XN, Huang Y, Wang W, Jing QL, Zhang CH, Qin PZ, et al. Effectiveness of inactivated SARS-CoV-2 vaccines against the Delta variant infection in Guangzhou: a test-negative case-control real-world study. *Emerg Microbes Infect.* 2021; 10: 1751–1759. <https://doi.org/10.1080/22221751.2021.1969291> PMID: 34396940
79. Obermeyer F, Jankowiak M, Barkas N, Schaffner SF, Pyle JD, Yurkovetskiy L, et al. Analysis of 6.4 million SARS-CoV-2 genomes identifies mutations associated with fitness. *Science.* 2022; 376: 1327–1332. <https://doi.org/10.1126/science.abm1208> PMID: 35608456
80. Liu Y, Rocklöv J. The reproductive number of the Delta variant of SARS-CoV-2 is far higher compared to the ancestral SARS-CoV-2 virus. *J Travel Med.* 2021; 28: taab124. <https://doi.org/10.1093/jtm/taab124> PMID: 34369565
81. Burki TK. Omicron variant and booster COVID-19 vaccines. *Lancet Respir Med.* 2022; 10: e17. [https://doi.org/10.1016/S2213-2600\(21\)00559-2](https://doi.org/10.1016/S2213-2600(21)00559-2) PMID: 34929158
82. Bundgaard H, Bundgaard JS, Raaschou-Pedersen DET, von Buchwald C, Todsén T, Norsk JB, et al. Effectiveness of adding a mask recommendation to other public health measures to prevent sars-cov-2 infection in danish mask wearers a randomized controlled trial. *Ann Intern Med.* 2021; 174: 335–343. <https://doi.org/10.7326/M20-6817> PMID: 33205991
83. Li X, Xu S, Yu M, Wang K, Tao Y, Zhou Y, et al. Risk factors for severity and mortality in adult COVID-19 inpatients in Wuhan. *J Allergy Clin Immunol.* 2020; 146: 110–118. <https://doi.org/10.1016/j.jaci.2020.04.006> PMID: 32294485
84. Nandy K, Salunke A, Pathak SK, Pandey A, Doctor C, Puj K, et al. Coronavirus disease (COVID-19): A systematic review and meta-analysis to evaluate the impact of various comorbidities on serious events. *Diabetes Metab Syndr Clin Res Rev.* 2020; 14: 1017–1025. <https://doi.org/10.1016/j.dsx.2020.06.064> PMID: 32634716
85. Zhang M, Wu J, Zhang X, Hu CH, Zhao ZP, Li C, et al. Prevalence and control of hypertension in adults in China, 2018. *Zhonghua liu xing bing xue za zhi.* 2021; 42: 1780–1789. <https://doi.org/10.3760/cma.j.cn112338-20210508-00379> PMID: 34814612
86. Bennett KE, Mullooly M, O'Loughlin M, Fitzgerald M, O'Donnell J, O'Connor L, et al. Underlying conditions and risk of hospitalisation, ICU admission and mortality among those with COVID-19 in Ireland: A national surveillance study. *Lancet Reg Heal—Eur.* 2021; 5: 100097. <https://doi.org/10.1016/j.lanepe.2021.100097> PMID: 33880459
87. Yuchang Z. A study of diabetes prevalence and disability life expectancy loss by province in China, 2005–2018. Shandong Univ thesis. 2021.
88. Qian KE; Chuanhua YU; Xiaoxue LIU; Haoyu WEN. The current status and trends of chronic kidney disease (CKD) burden in China based on GBD Data. *J Public Heal Prev Med.* 2021; 6: 1–5.
89. Denova-Gutiérrez E, Lopez-Gatell H, Alomia-Zegarra JL, López-Ridaura R, Zaragoza-Jimenez CA, Dyer-Leal DD, et al. The Association of Obesity, Type 2 Diabetes, and Hypertension with Severe Coronavirus Disease 2019 on Admission Among Mexican Patients. *Obesity.* 2020; 28: 1826–1832. <https://doi.org/10.1002/oby.22946> PMID: 32610364
90. Zhang L, Wang Z, Wang X, Chen Z, Shao L, Tian Y, et al. Prevalence of overweight and obesity in China: Results from a cross-sectional study of 441 thousand adults, 2012–2015. *Obes Res Clin Pract.* 2020; 14: 119–126. <https://doi.org/10.1016/j.orcp.2020.02.005> PMID: 32139330
91. Pan X-F, Wang L, Pan A. Epidemiology and determinants of obesity in China. *Lancet Diabetes Endocrinol.* 2021; 9: 373–392. [https://doi.org/10.1016/S2213-8587\(21\)00045-0](https://doi.org/10.1016/S2213-8587(21)00045-0) PMID: 34022156
92. Robilotti E V., Babady NE, Mead PA, Rolling T, Perez-Johnston R, Bernardes M, et al. Determinants of COVID-19 disease severity in patients with cancer. *Nat Med.* 2020; 26: 1218–1223. <https://doi.org/10.1038/s41591-020-0979-0> PMID: 32581323
93. Yin P, Wu J, Wang L, Luo C, Ouyang L, Tang X, et al. The Burden of COPD in China and Its Provinces: Findings From the Global Burden of Disease Study 2019. *Front public Heal.* 2022; 10: 859499. <https://doi.org/10.3389/fpubh.2022.859499> PMID: 35757649
94. Lin J, Wang W, Chen P, Zhou X, Wan H, Yin K, et al. Prevalence and risk factors of asthma in mainland China: The CARE study. *Respir Med.* 2018; 137: 48–54. <https://doi.org/10.1016/j.rmed.2018.02.010> PMID: 29605212

95. Huang K, Yang T, Xu J, Yang L, Zhao J, Zhang X, et al. Prevalence, risk factors, and management of asthma in China: a national cross-sectional study. *Lancet*. 2019; 394: 407–418. [https://doi.org/10.1016/S0140-6736\(19\)31147-X](https://doi.org/10.1016/S0140-6736(19)31147-X) PMID: 31230828
96. Li X, Song P, Zhu Y, Lei H, Chan KY, Campbell H, et al. The disease burden of childhood asthma in China: a systematic review and meta-analysis. *J Glob Health*. 2020; 10: 010801. <https://doi.org/10.7189/jogh.10.01081> PMID: 32257166
97. Li M, Wang ZQ, Zhang L, Zheng H, Liu DW, Zhou MG. Burden of Cirrhosis and Other Chronic Liver Diseases Caused by Specific Etiologies in China, 1990–2016: Findings from the Global Burden of Disease Study 2016. *Biomed Environ Sci*. 2020; 33: 1–10. <https://doi.org/10.3967/bes2020.001> PMID: 32029053
98. Zhang L, Fan ZF, Liu DW, Zhou MG, Wang ZQ, Li M. Trend analysis on the disease burden related to cirrhosis and other chronic liver diseases caused by hepatitis B, in China, from 1990 to 2016. *Zhonghua Liu Xing Bing Xue Za Zhi*. 2020; 41: 173–177. <https://doi.org/10.3760/cma.j.issn.0254-6450.2020.02.007> PMID: 32164125
99. Zheng R, Zhang S, Zeng H, Wang S, Sun K, Chen R, et al. Cancer incidence and mortality in China, 2016. *J Natl Cancer Cent*. 2022; 2: 1–9. <https://doi.org/10.1016/j.jncc.2022.02.002>